

2.3 Number of light neutrino generations

In the Standard Model:

$$\Gamma_Z = \Gamma_{had} + 3 \cdot \underbrace{\Gamma_\ell + N_\nu \cdot \Gamma_\nu}_{\text{invisible}} \rightarrow \left\{ \begin{array}{l} e^+ e^- \rightarrow Z \rightarrow \nu_e \bar{\nu}_e \\ e^+ e^- \rightarrow Z \rightarrow \nu_\mu \bar{\nu}_\mu \\ e^+ e^- \rightarrow Z \rightarrow \nu_\tau \bar{\nu}_\tau \end{array} \right.$$

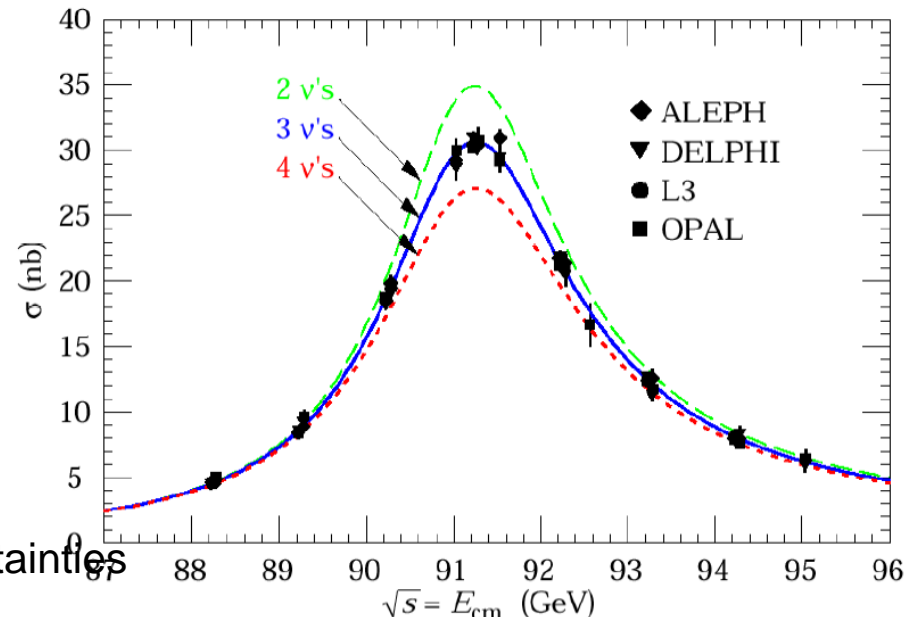
$$\boxed{\Gamma_{inv} = 0.4990 \pm 0.0015 \text{ GeV}}$$

To determine the number of light neutrino generations:

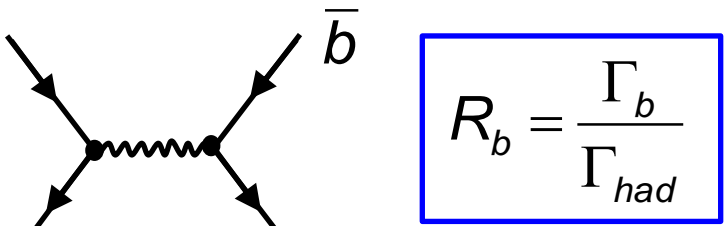
$$N_\nu = \frac{\Gamma_{inv}}{\Gamma_{\nu,SM}} = \underbrace{\left(\frac{\Gamma_{inv}}{\Gamma_\ell} \right)_{exp}}_{5.9431 \pm 0.0163} \cdot \underbrace{\left(\frac{\Gamma_\ell}{\Gamma_\nu} \right)_{SM}}_{=1/1.991 \pm 0.001} \quad (\text{small theo. uncertainties from } m_{top}, M_H)$$

$$\boxed{N_\nu = 2.9840 \pm 0.0082}$$

No room for new physics: $Z \rightarrow \text{new}$



Heavy Quark production

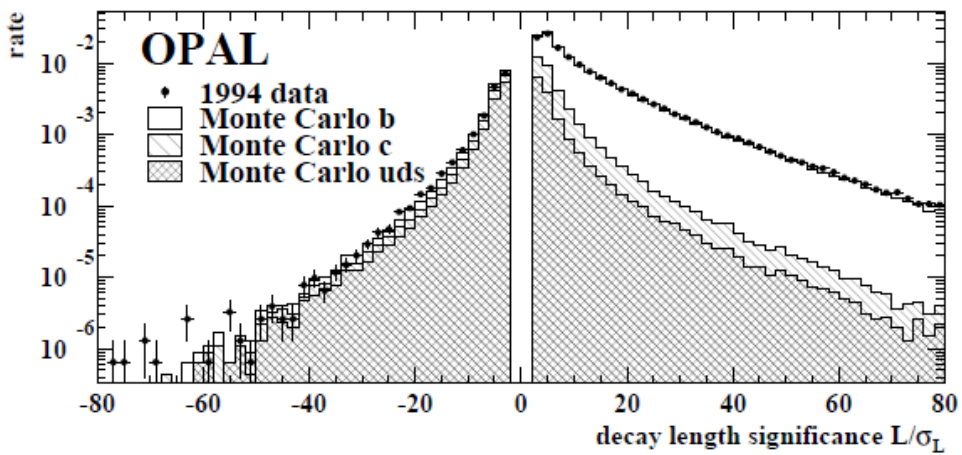
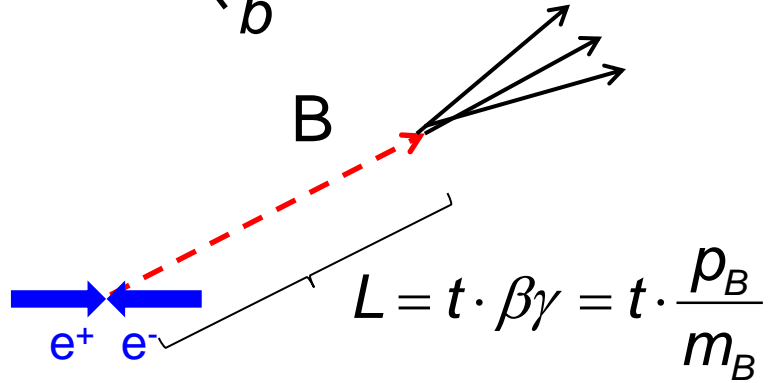


$$R_b = \frac{\Gamma_b}{\Gamma_{had}}$$

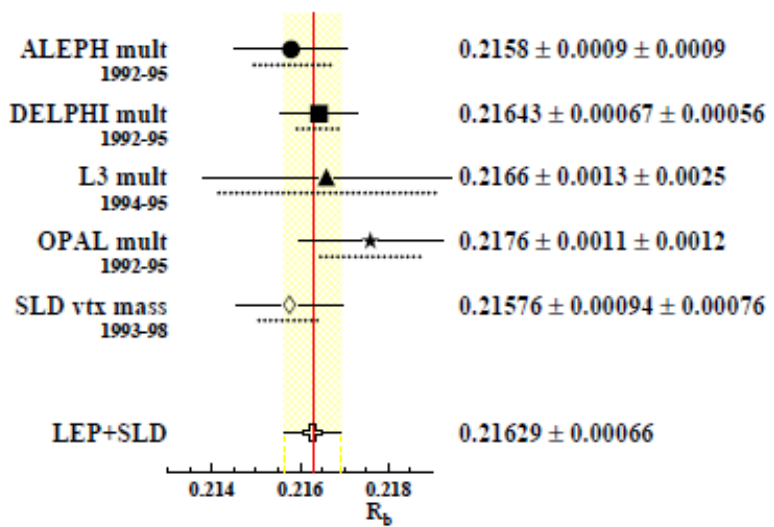
Identification of b-Quark events:

b-quarks hadronize to b-hadrons (B 's, Λ_b) with typical lifetime of ~ 1 ps \rightarrow decay length

Use displaced “2nd” B decay vertex as signature.



Significance = L / error



2.4 Lepton couplings to the Z boson

In the following ignore the difference between chirality and helicity:
good approximation as leptons are produced with energies \gg mass.

Z boson couples differently to LH and RH leptons:

$$\left| g_L = \frac{1}{2}(g_V + g_A) \right| > \left| g_R = \frac{1}{2}(g_V - g_A) \right|$$

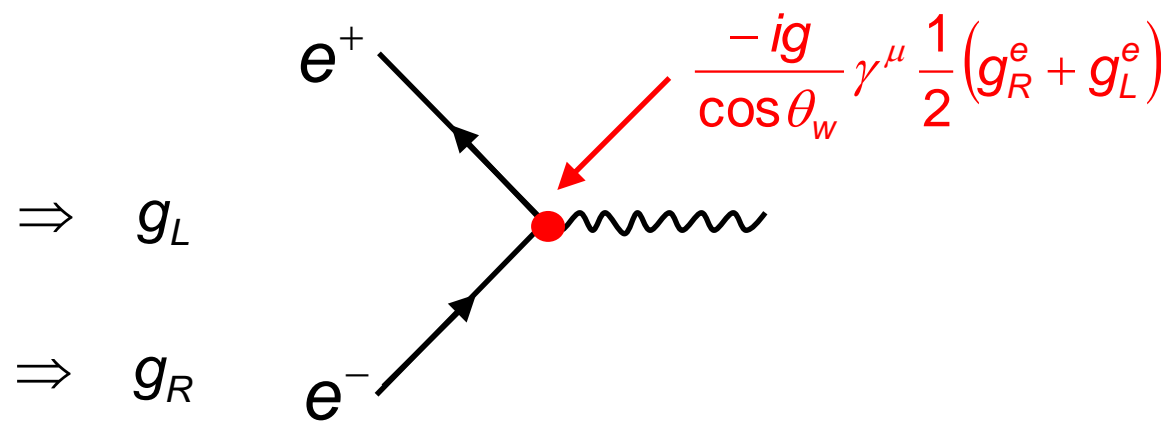
→ Coupling to LH leptons stronger

Z produced in e^+e^- collisions is polarized.

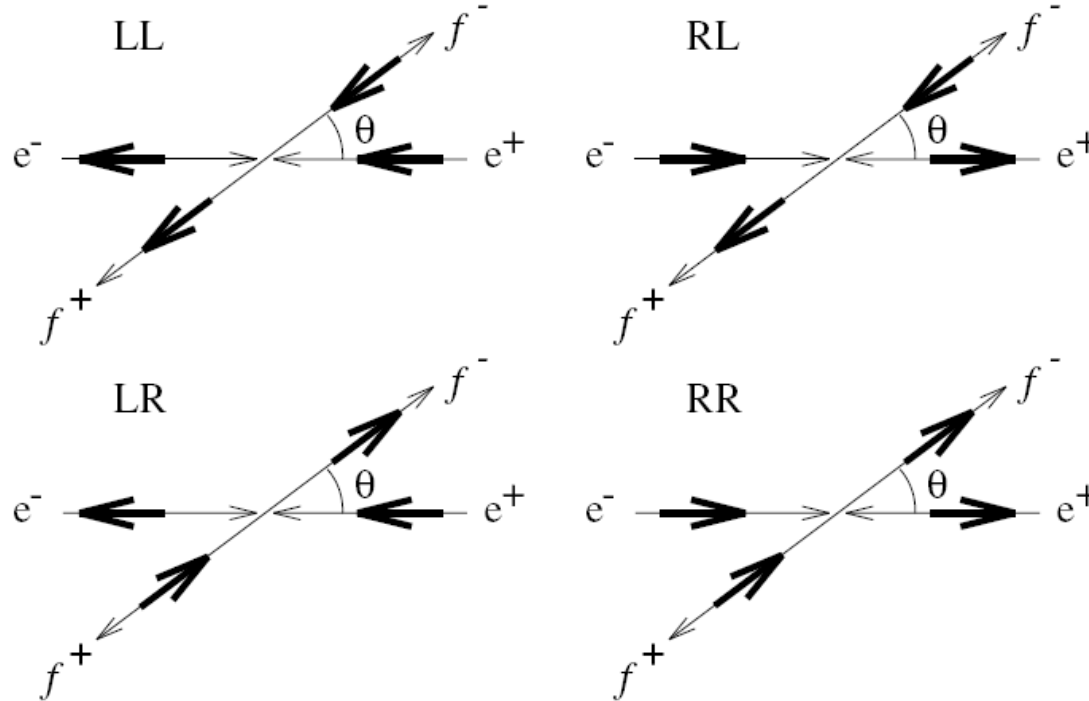
Experimental configuration:

$$e^- \xrightarrow{\text{blue}} \xleftarrow{\text{red}} e^+ \Rightarrow g_L$$

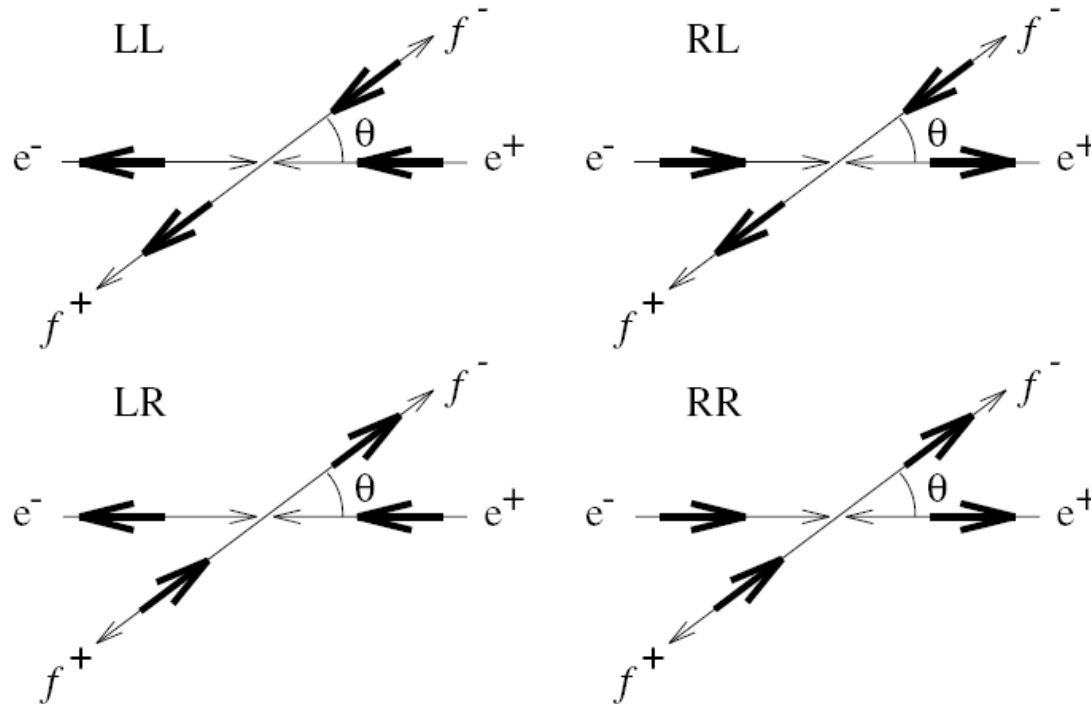
$$\xrightarrow{\text{red}} \xrightarrow{\text{blue}} e^- \Rightarrow g_R$$



Instead of measuring the spin averaged transition amplitudes try to decompose the different “helicity” components to the cross section:



Chirality		amplitude	
e	f		
L	L	$\mathcal{M}_{LL} \propto g_L^f g_L^e d_{11}^1(\theta)$	$\propto g_L^f g_L^e (1 + \cos \theta)$
R	L	$\mathcal{M}_{RL} \propto g_L^f g_R^e d_{11}^1(\theta + \pi)$	$\propto g_L^f g_R^e (1 - \cos \theta)$
L	R	$\mathcal{M}_{LR} \propto g_R^f g_L^e d_{11}^1(\theta + \pi)$	$\propto g_R^f g_L^e (1 - \cos \theta)$
R	R	$\mathcal{M}_{RR} \propto g_R^f g_R^e d_{11}^1(\theta)$	$\propto g_R^f g_R^e (1 + \cos \theta)$



Observables:

$$\sigma_F = \sigma_{LL} + \sigma_{RR}$$

$$\sigma_B = \sigma_{RL} + \sigma_{LR}$$

$$A_{FB} = \frac{\sigma_F - \sigma_B}{\sigma_F + \sigma_B}$$

Forward-backward asym. (final)

$$\sigma_L = \sigma_{LL} + \sigma_{LR}$$

$$\sigma_R = \sigma_{RL} + \sigma_{RR}$$

$$A_{LR} = \frac{\sigma_L - \sigma_R}{\sigma_L + \sigma_R}$$

Left right asym. (initial)

$$\sigma_- = \sigma_{LL} + \sigma_{RL}$$

$$\sigma_+ = \sigma_{RR} + \sigma_{LR}$$

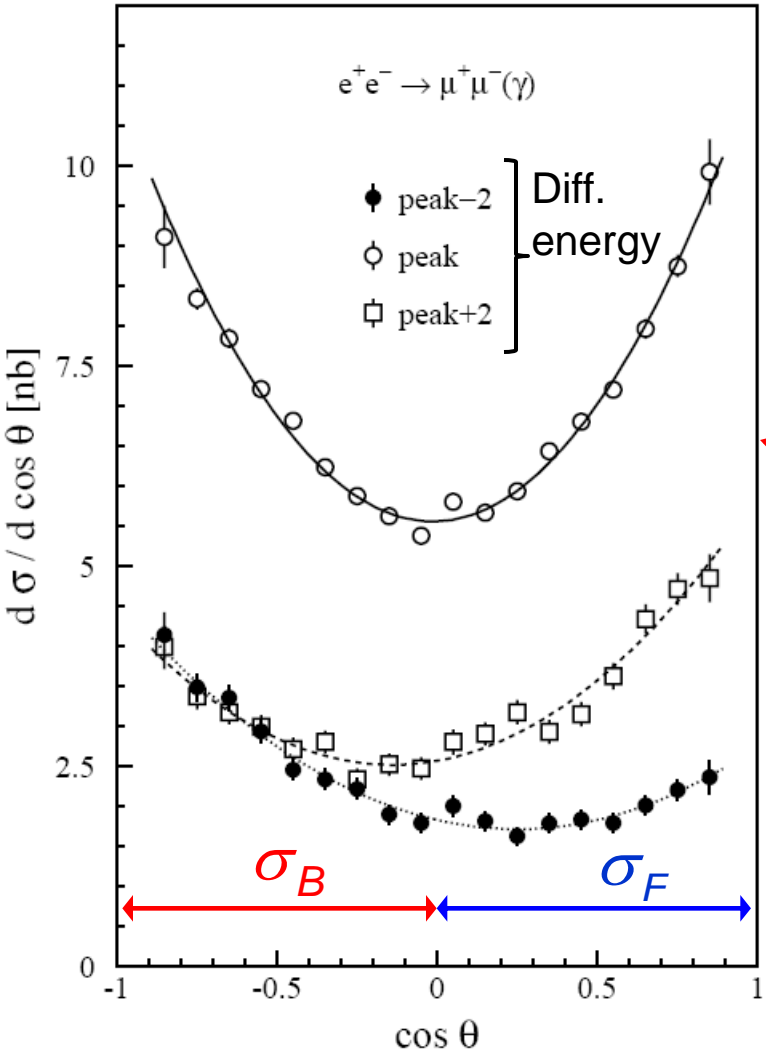
$$\mathcal{P}_f = \frac{\sigma_+ - \sigma_-}{\sigma_+ + \sigma_-}$$

fermion polarization (final)

2.5 Forward-backward asymmetry and fermion couplings to Z

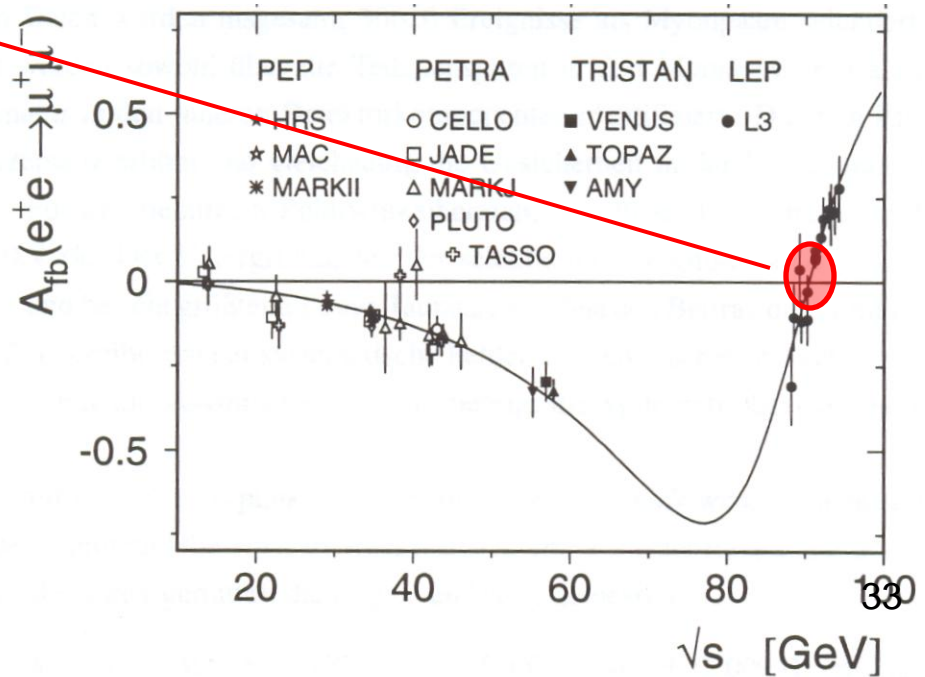
$e^+ e^- \rightarrow Z \rightarrow \mu^+ \mu^-$

$$\frac{d\sigma}{d\cos\theta} \sim (1 + \cos^2\theta) + \frac{8}{3} A_{FB} \cos\theta$$



$$\text{with } A_{FB} = \frac{\sigma_F - \sigma_B}{\sigma_F + \sigma_B}$$

$$\sigma_{F(B)} = \int_0^{1(0)} \frac{d\sigma}{d\cos\theta} d\cos\theta$$



Angular distribution: (see above)

$$F_{\gamma Z}(\cos \theta) = \frac{Q_e Q_\mu}{4 \sin^2 \theta_W \cos^2 \theta_W} [2g_V^e g_V^\mu (1 + \cos^2 \theta) + 4g_A^e g_A^\mu \cos \theta]$$

$$F_Z(\cos \theta) = \frac{1}{16 \sin^4 \theta_W \cos^4 \theta_W} [(g_V^{e2} + g_A^{e2})(g_V^{\mu2} + g_A^{\mu2}) (1 + \cos^2 \theta) + 8g_V^e g_A^e g_V^\mu g_A^\mu \cos \theta]$$

Forward-backward asymmetry A_{FB}

- Away from the resonance large \rightarrow interference term dominates

$$A_{FB} \sim g_A^e g_A^f \cdot \frac{s(s - M_Z^2)}{(s - M_Z^2)^2 + M_Z^2 \Gamma_Z^2} \quad \rightarrow \text{large}$$

- At the Z pole: Interference = 0 (see energy dependence of interference term)

$$A_{FB} = 3 \cdot \frac{g_V^e g_A^e}{(g_V^e)^2 + (g_A^e)^2} \cdot \frac{g_V^\mu g_A^\mu}{(g_V^\mu)^2 + (g_A^\mu)^2}$$

\rightarrow very small because g_V^e small in SM

Asymmetrie at the Z pole

$$A_{FB} \sim g_A^e g_V^e g_A^f g_V^f$$

Cross section at the Z pole

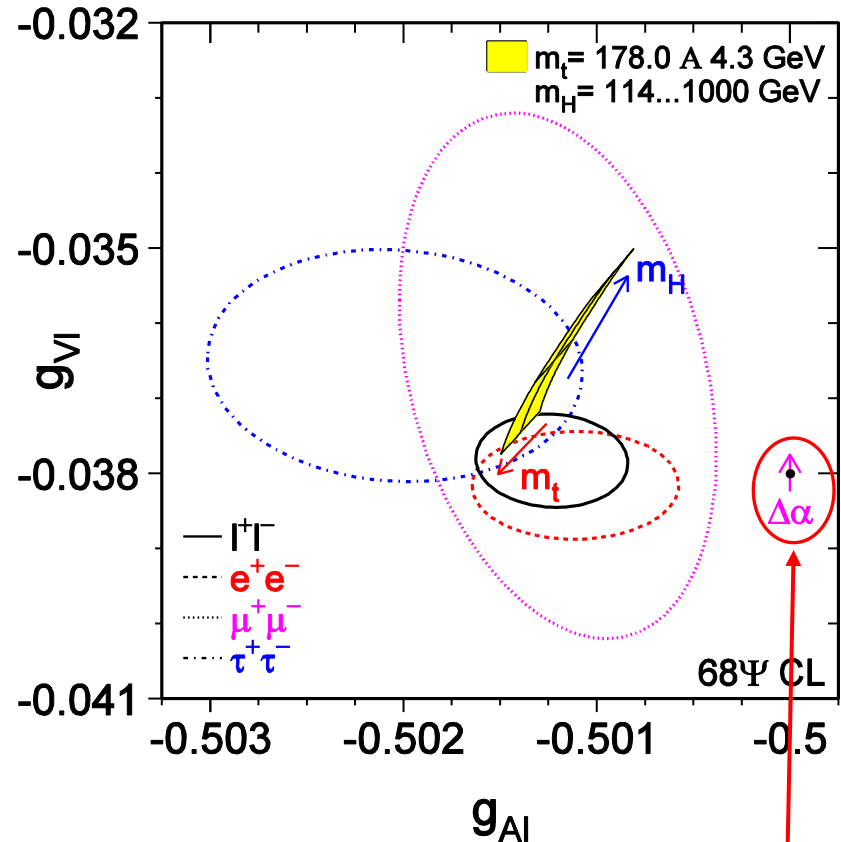
$$\sigma_Z \sim [(g_V^e)^2 + (g_A^e)^2][(g_V^\mu)^2 + (g_A^\mu)^2]$$



Lepton asymmetries together with lepton pair cross sections allow the determination of the lepton couplings g_A and g_V .



Good agreement between the 3 lepton species confirms “lepton universality”



Lowest order SM prediction:

$$g_V = T_3 - 2q \sin^2 \theta_W \quad g_A = T_3$$

Deviation from lowest order SM prediction is an effect of higher-order electroweak corrections.

2.6 Polarization of final state leptons: tau pol.

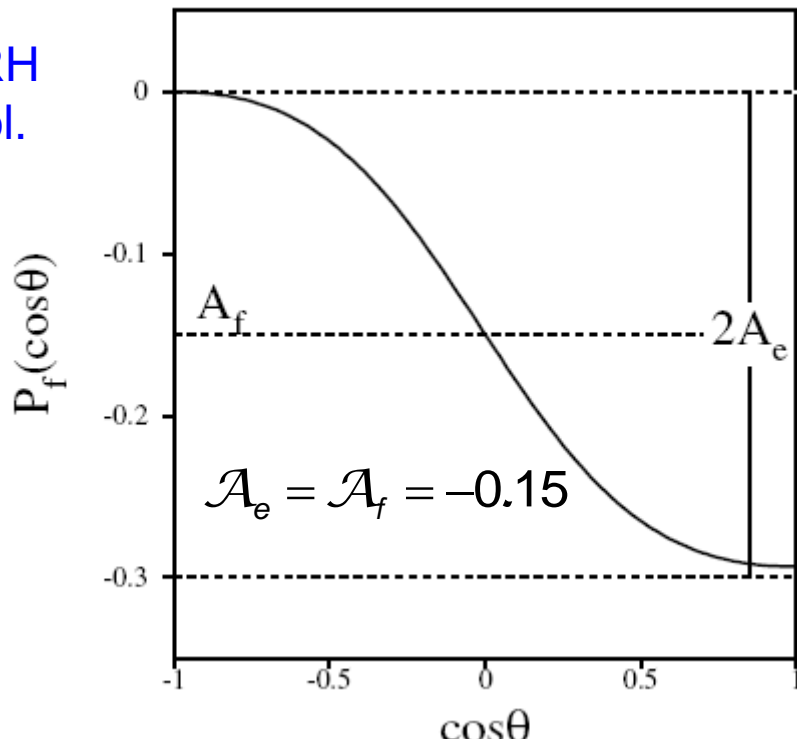
$$\mathcal{P}_f(\cos\theta) = \frac{\frac{d\sigma_+}{d\cos\theta} - \frac{\sigma_-}{d\cos\theta}}{\frac{d\sigma_+}{d\cos\theta} + \frac{\sigma_-}{d\cos\theta}}$$

$\sigma_{L(R)} = LH/RH$
fermion pol.

$$\mathcal{P}_f(\cos\theta) = \frac{\mathcal{A}_f(1+\cos^2\theta) + 2\mathcal{A}_e \cos\theta}{(1+\cos^2\theta) + 8/3 A_{FB} \cos\theta}$$

with $\mathcal{A}_i = \frac{2g_V^i g_A^i}{(g_V^i)^2 + (g_A^i)^2}$

$$\mathcal{P}_\ell \approx -2 \frac{2g_V^\ell}{g_A^\ell} = -2(1 - 4\sin^2\theta_w)$$

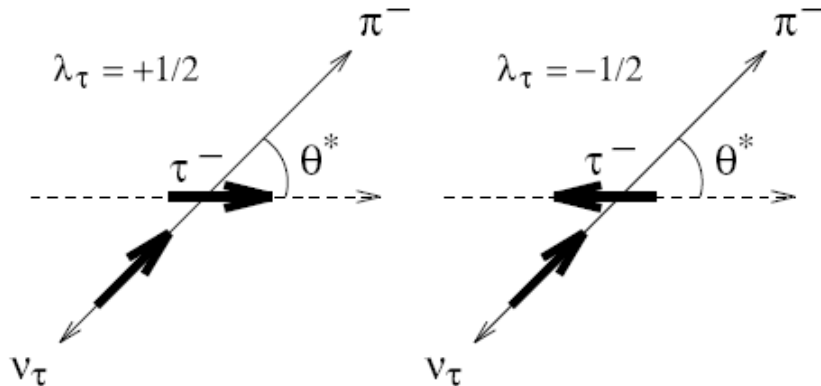


($\cos\theta$ is the fermion scattering angle)

Lepton polarization measures directly $\sin^2\theta_w$.
The only lepton for which polarization can be measured at LEP is the tau!

Experimental Method to measure tau polarization:

$$\tau^- \rightarrow \pi^- \nu_\tau \quad \text{Spin } \frac{1}{2} \rightarrow \text{Spin } \frac{1}{2} + \text{Spin } 0$$



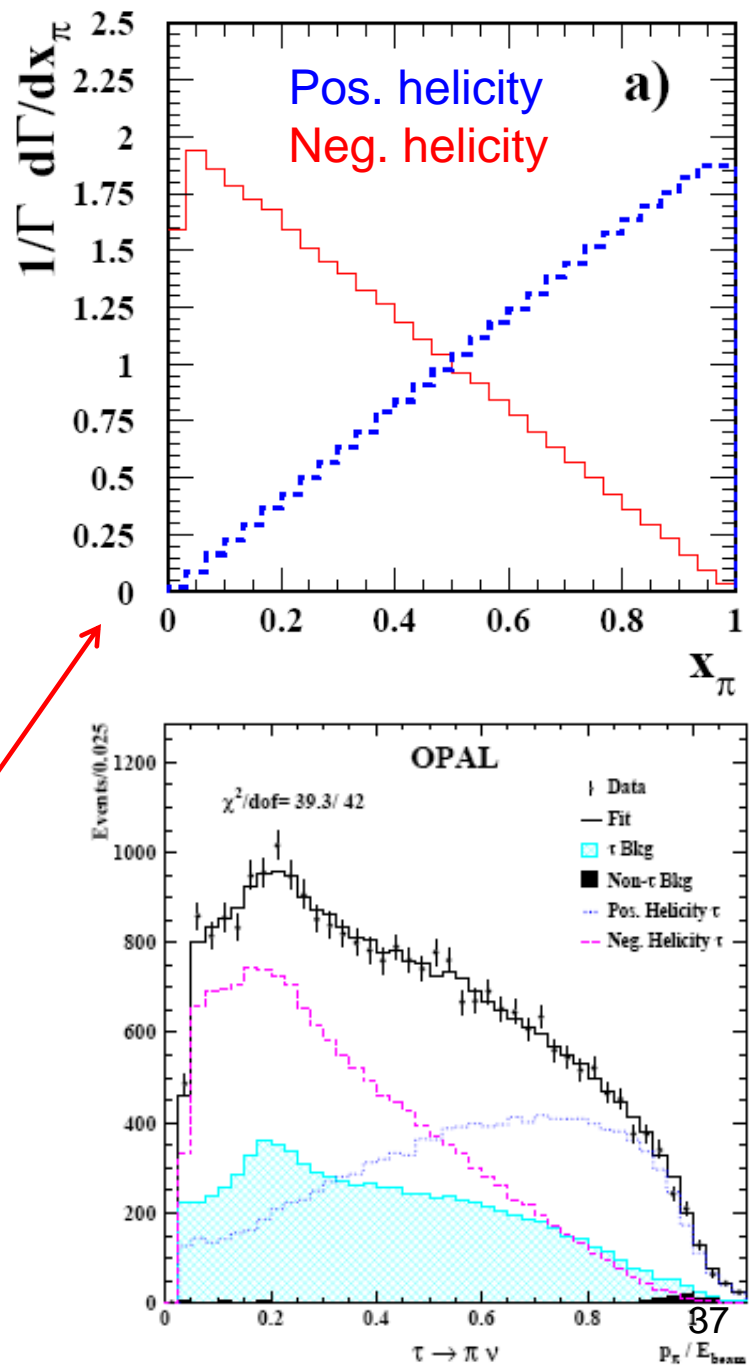
$$\frac{1}{\Gamma} \frac{d\Gamma}{d \cos \theta^*} = \frac{1}{2} (1 + \mathcal{P}_\tau \cos \theta^*)$$



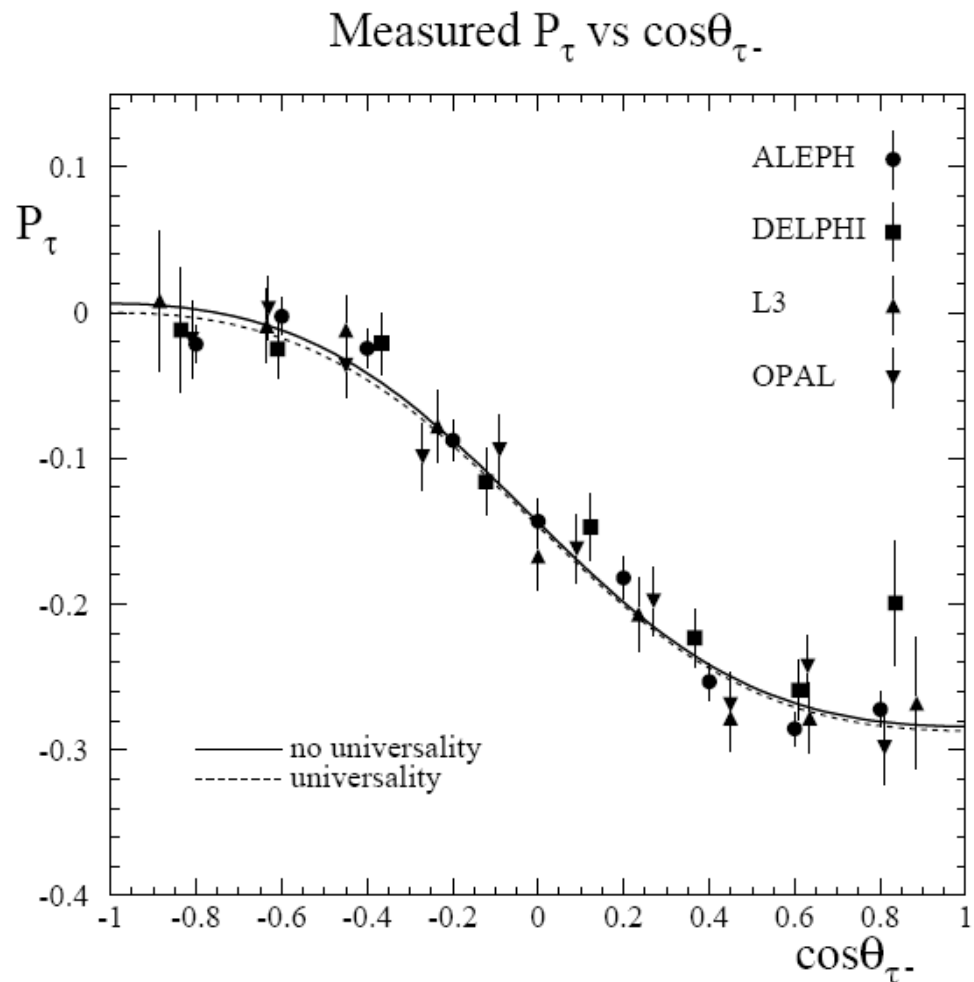
Boost into lab frame

$$\boxed{\frac{1}{\Gamma} \frac{d\Gamma}{dx_\pi} = 1 + \mathcal{P}_\tau (2x_\pi - 1) \quad x_\pi = E_\pi / E_\tau}$$

Fit of the two theoretical distribution to data yields the polarization: ~ 0.15



Measured Tau Polarization



$$\mathcal{A}_\tau = 0.1439 \pm 0.0043$$

$$\mathcal{A}_e = 0.1498 \pm 0.0049$$

$$\mathcal{A}_\ell = 0.1465 \pm 0.0033$$

$$\sin^2 \theta_w^{eff} = 0.23159 \pm 0.00041$$

[hep-ex/0509008](#)

2.7 Left-Right Asymmetry at SLC

Measure cross section σ_L (σ_R) for LH (RH) initial state electrons:

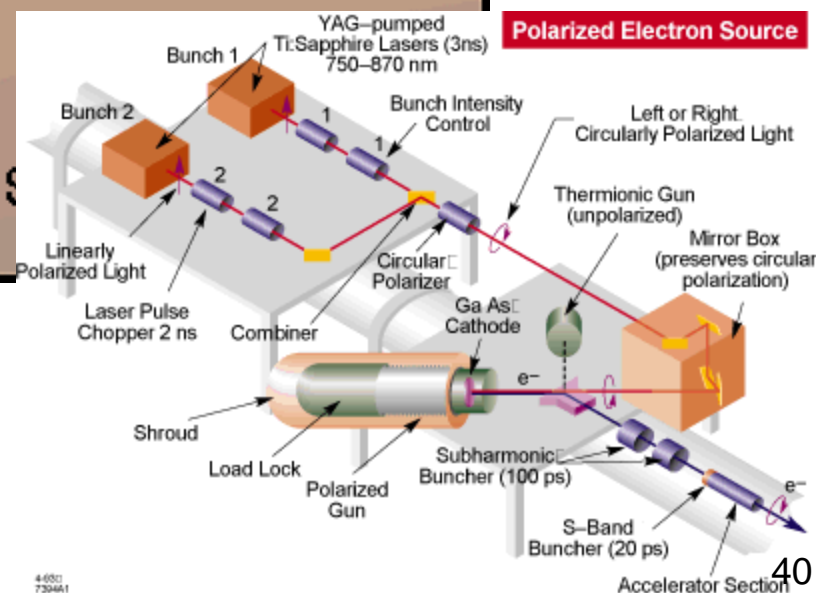
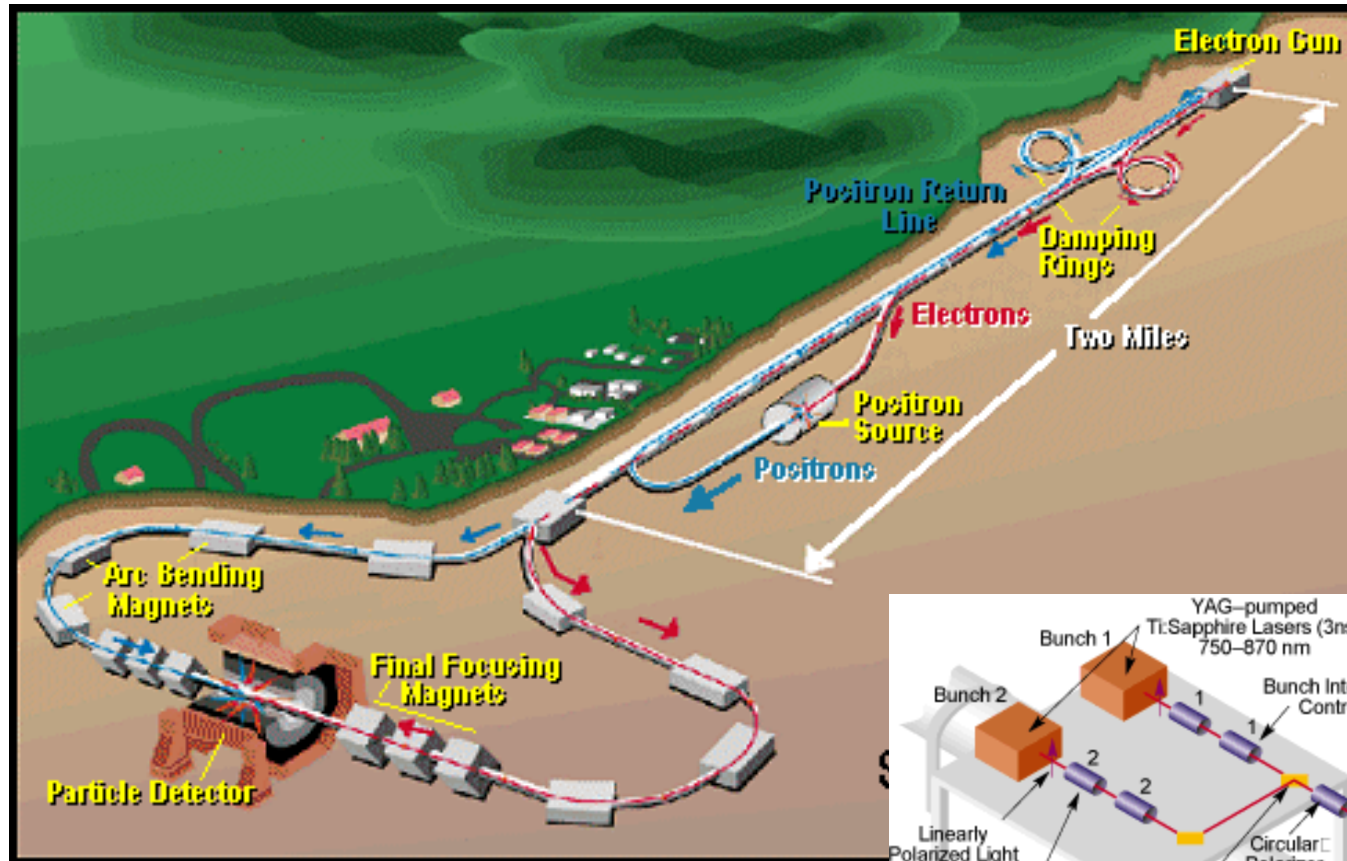
$$A_{LR} = \frac{1}{\mathcal{P}_e} \frac{\sigma_L^f - \sigma_R^f}{\sigma_L^f + \sigma_R^f}$$

$$A_{LR} = \frac{2g_V^e g_A^e}{(g_V^e)^2 + (g_A^e)^2} = \frac{2(1 - 4 \sin^2 \theta_w)}{1 + (1 - 4 \sin^2 \theta_w)^2}$$

Polarization of
electron beam:
 $P \sim 70 - 80\%$

Powerful determination of $\sin^2 \theta_w$.
Requires longitudinal polarization of colliding beams

SLAC Linear Collider



Typical beam polarization of 70%.

Precise determination of beam polarization using a Compton Polarimeter

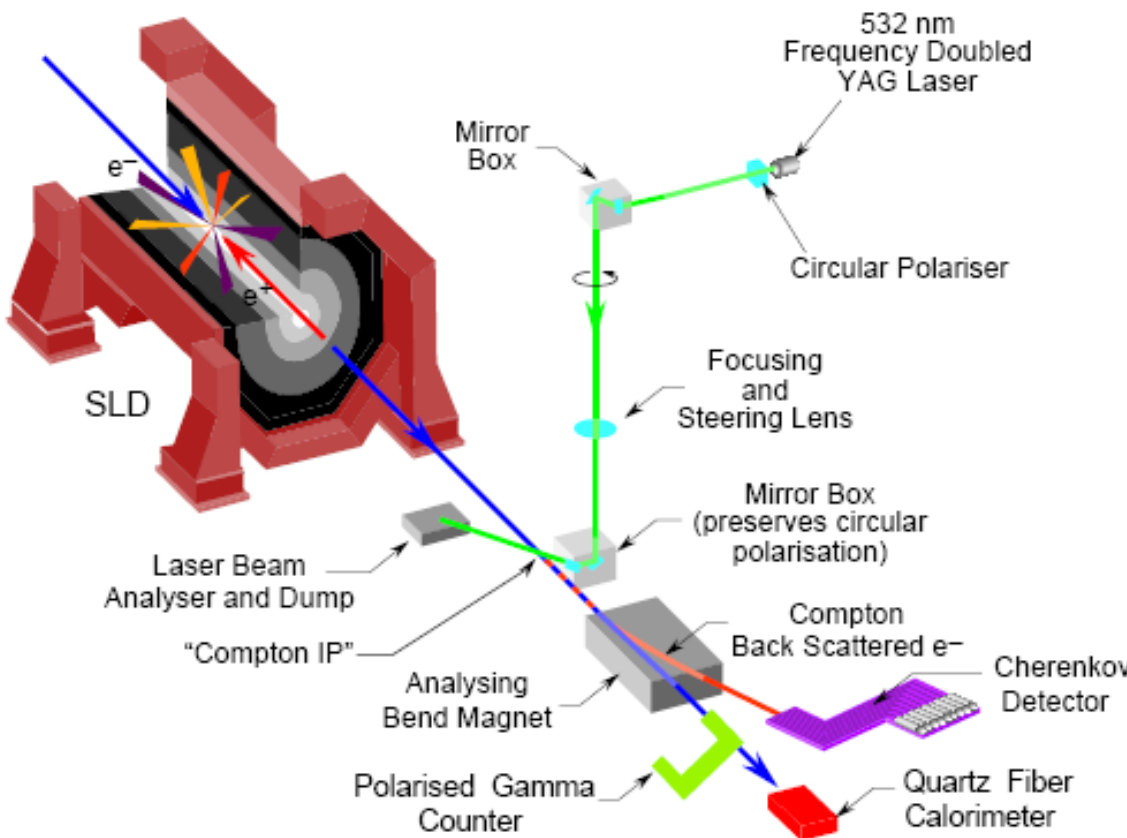
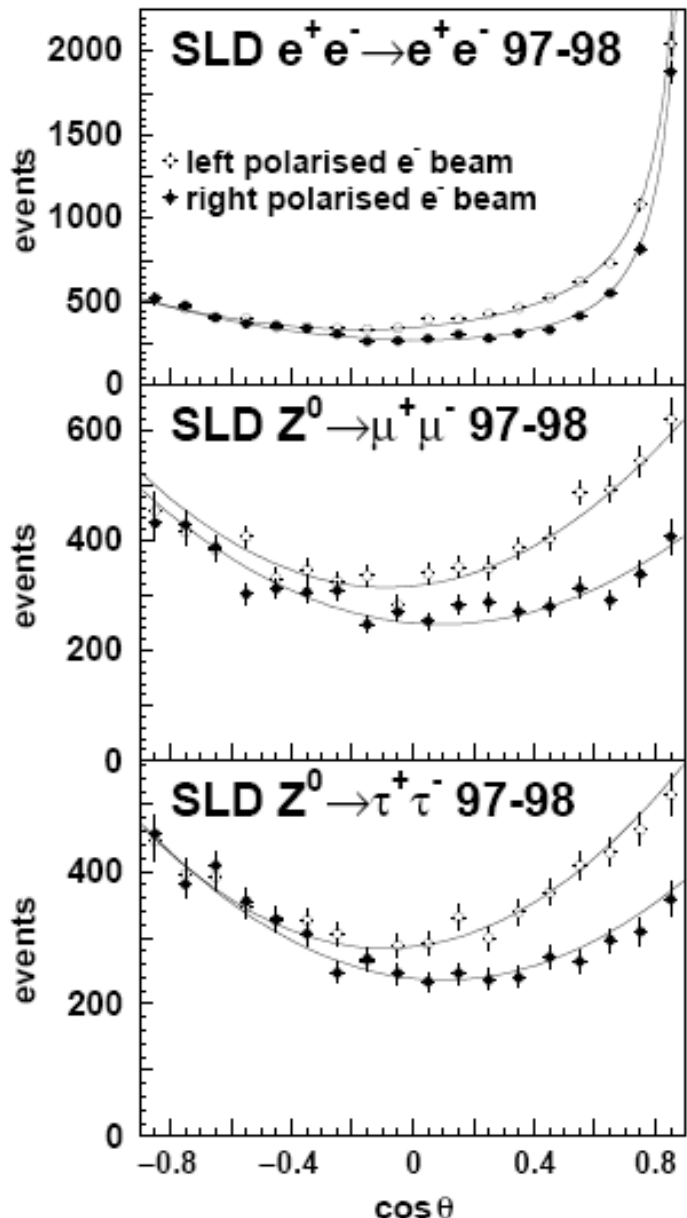


Figure 3.1: A conceptual diagram of the SLD Compton Polarimeter. The laser beam, consisting of 532 nm wavelength 8 ns pulses produced at 17 Hz and a peak power of typically 25 MW, were circularly polarised and transported into collision with the electron beam at a crossing angle of 10 mrad approximately 30 meters from the IP. Following the laser/electron-beam collision, the electrons and Compton-scattered photons, which are strongly boosted along the electron beam direction, continue downstream until analysing bend magnets deflect the Compton-scattered electrons into a transversely-segmented Cherenkov detector. The photons continue undeflected and are detected by a gamma counter (PGC) and a calorimeter (QFC) which are used to cross-check the polarimeter calibration.

Leptonic final states:



SLD

Asymmetry
clearly seen for
LH and RH
cross section.

SLD

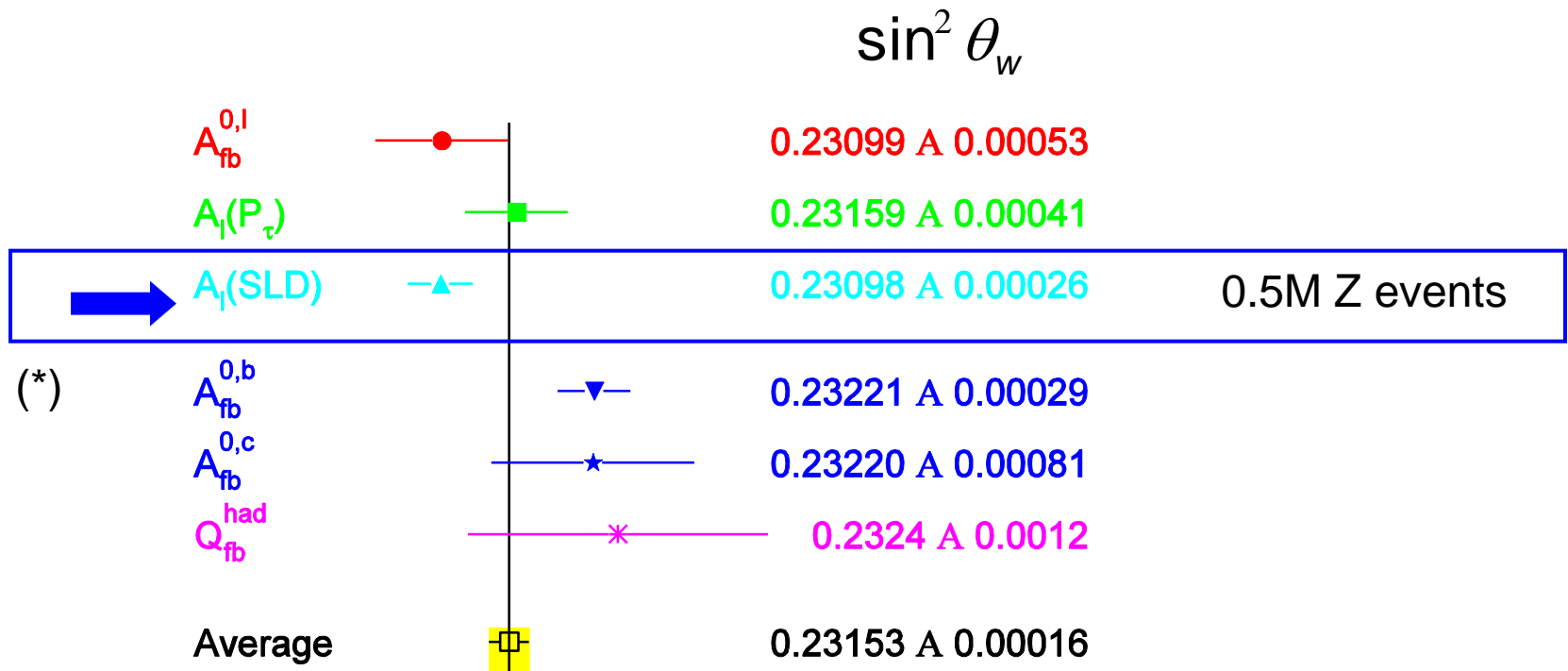
All data:

$$A_{LR} = 0.1513 \pm 0.0021$$

$$\sin^2 \theta_W = 0.23098 \pm 0.00026$$

With 0.5×10^6
Z-decays

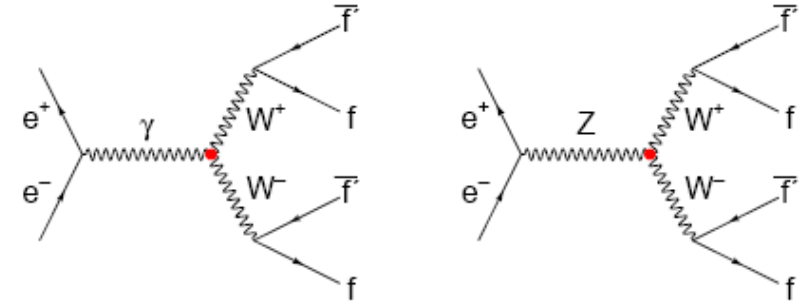
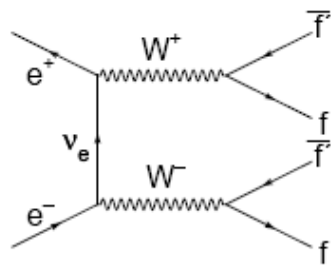
SLD versus $4 \times 4.5 \times 10^6$ Z-decays at LEP



(*) similar to R_b one can also determine the forward-backward asymmetry for bb-events.

3. Precision tests of the W sector (LEP2 and Tevatron)

$$e^+ e^- \rightarrow WW \rightarrow f\bar{f}f\bar{f}$$



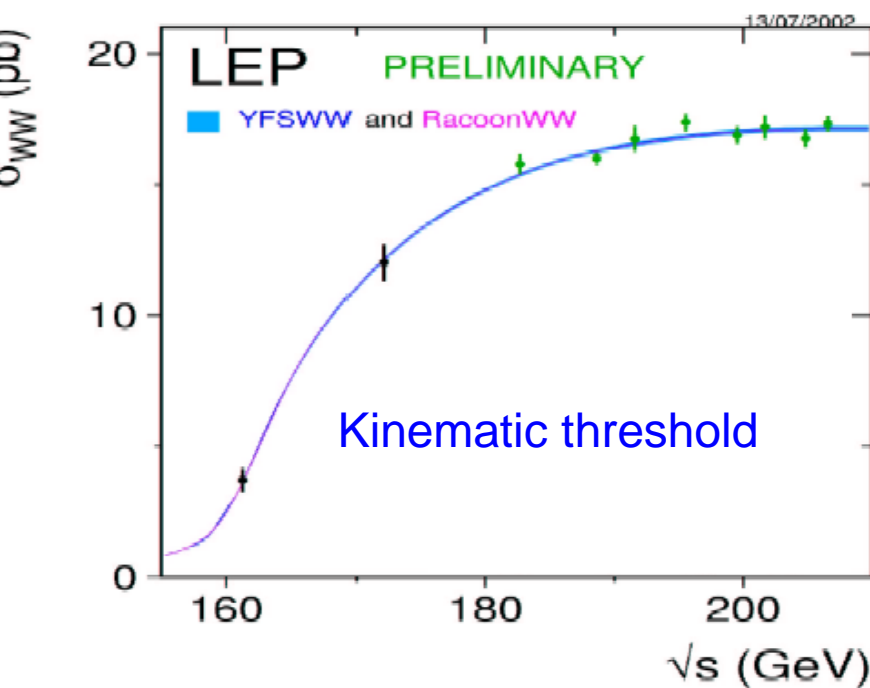
↑ ~10K WW events / experiment

Threshold behavior of the cross section (kinematics, phase space) for $ee \rightarrow WW$ production:

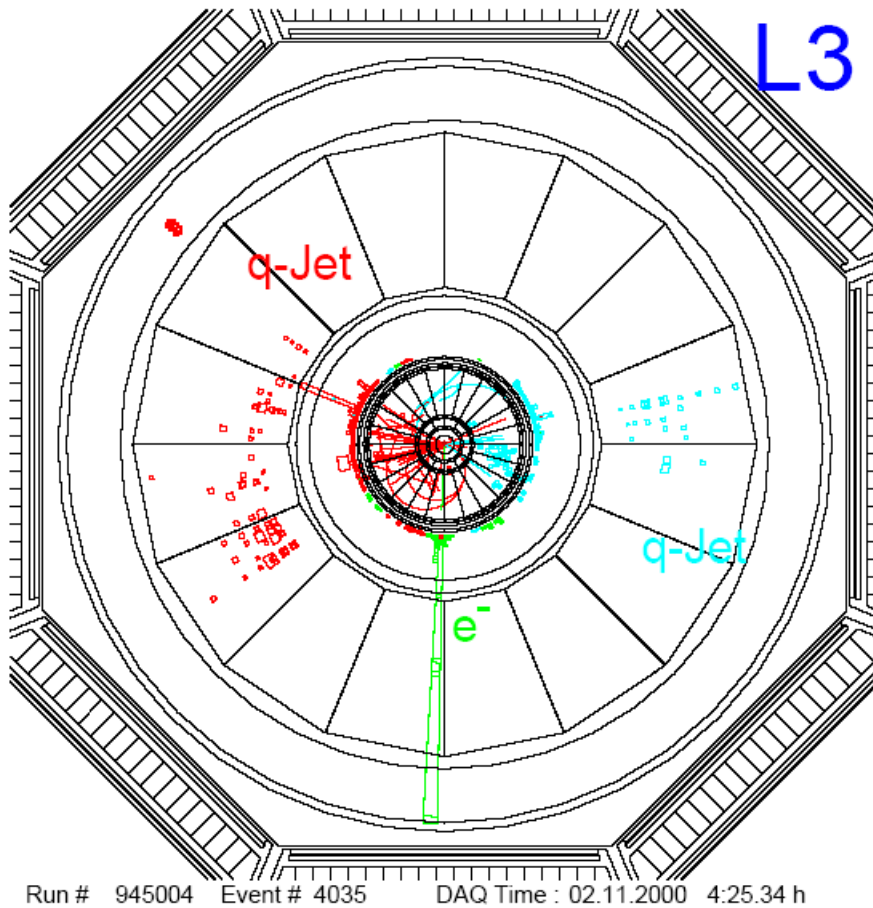


Phase space factor = $f(M_W, \sqrt{s})$:

→ Allows determination of M_W

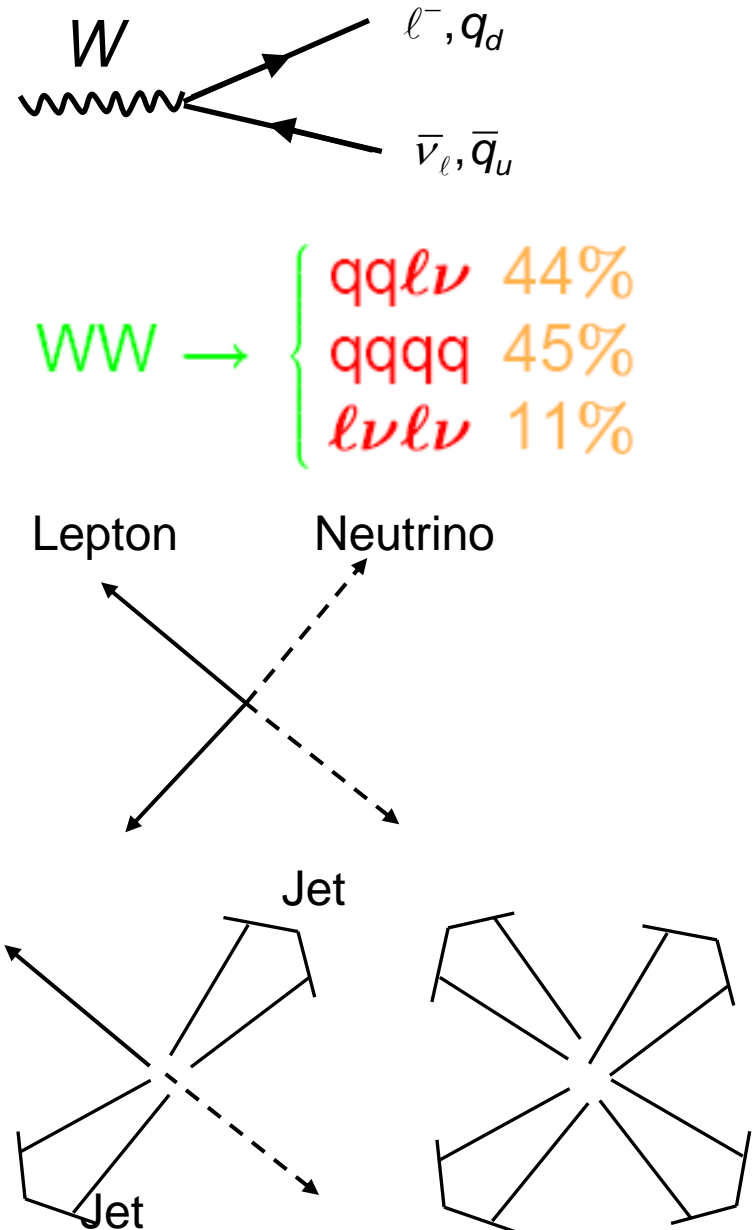


W decays

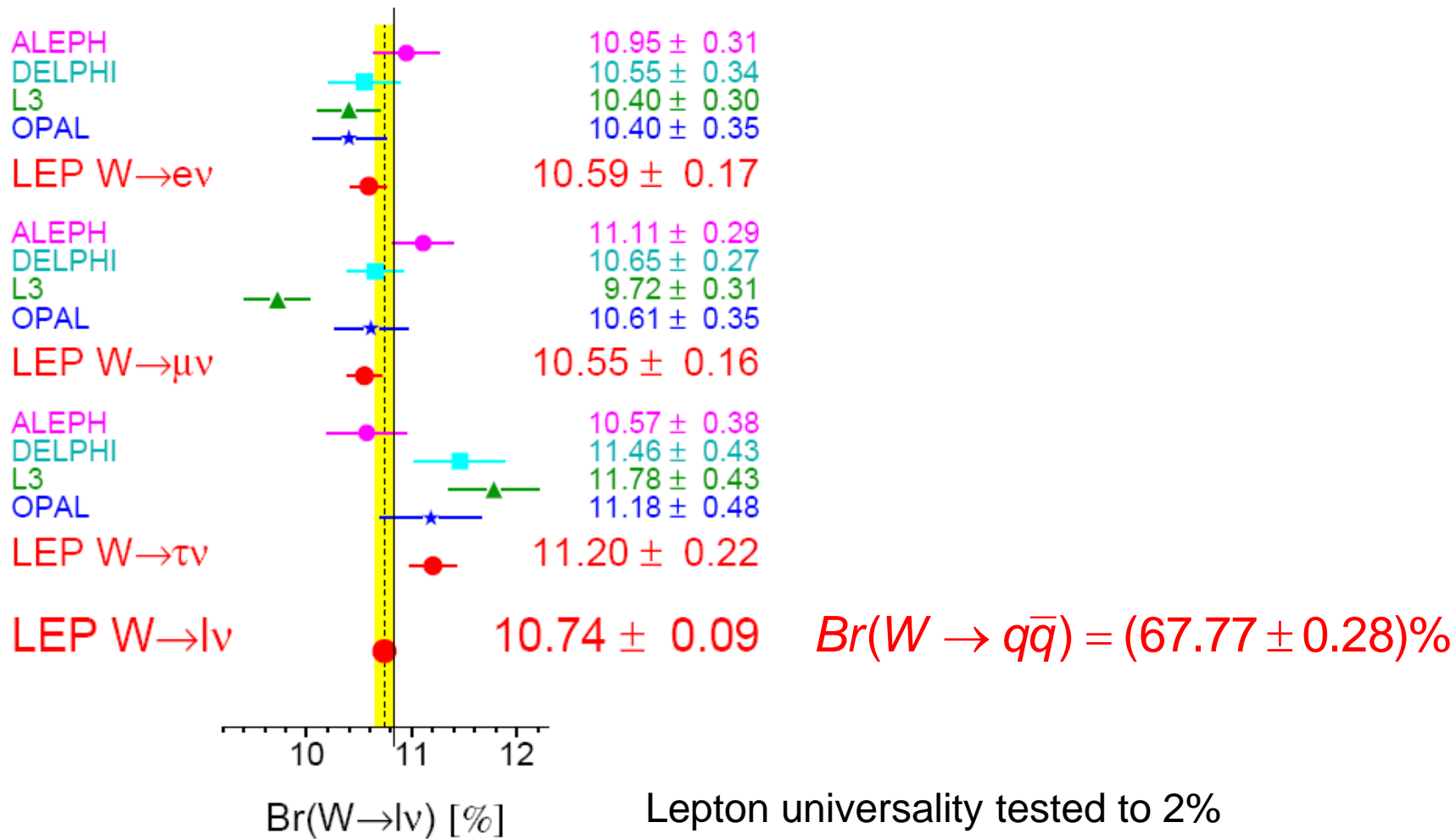


Easiest signature for a mass measurement:

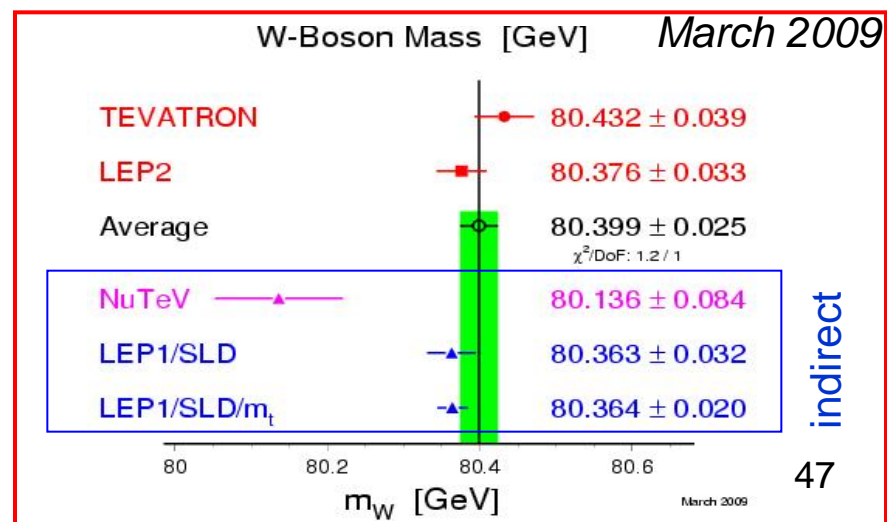
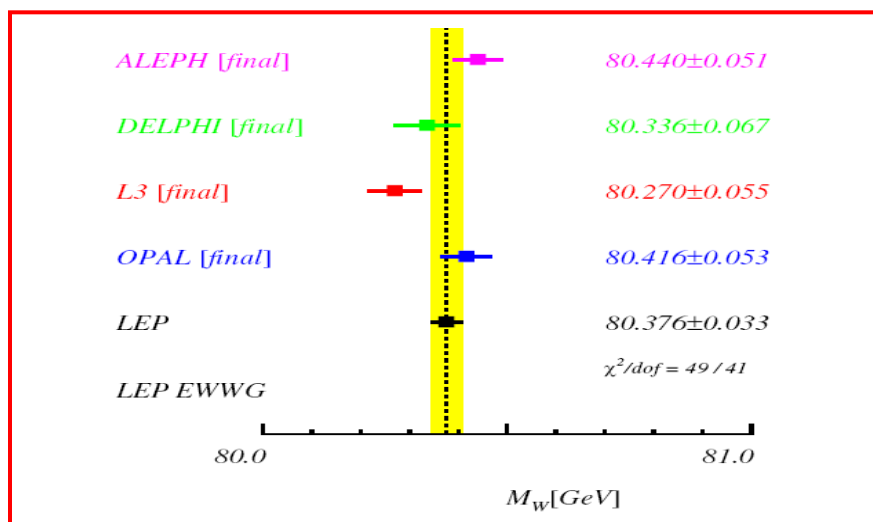
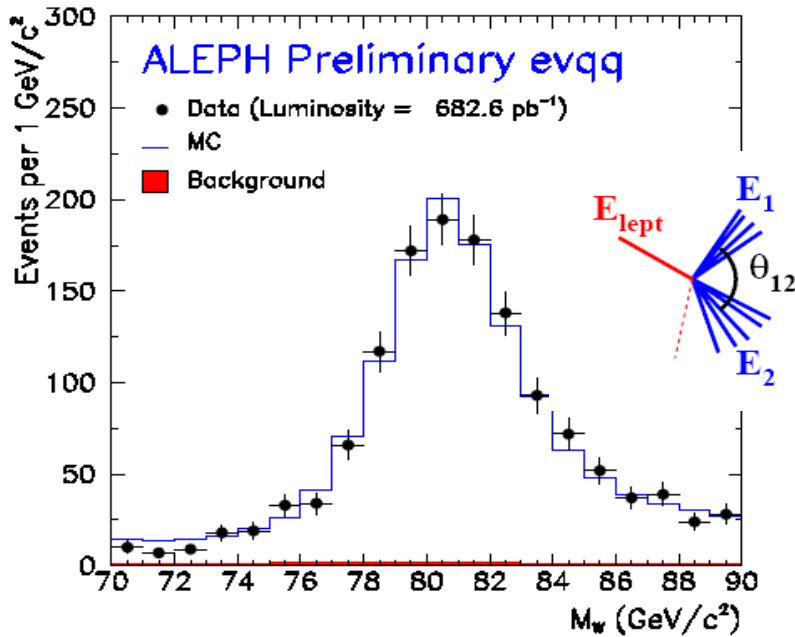
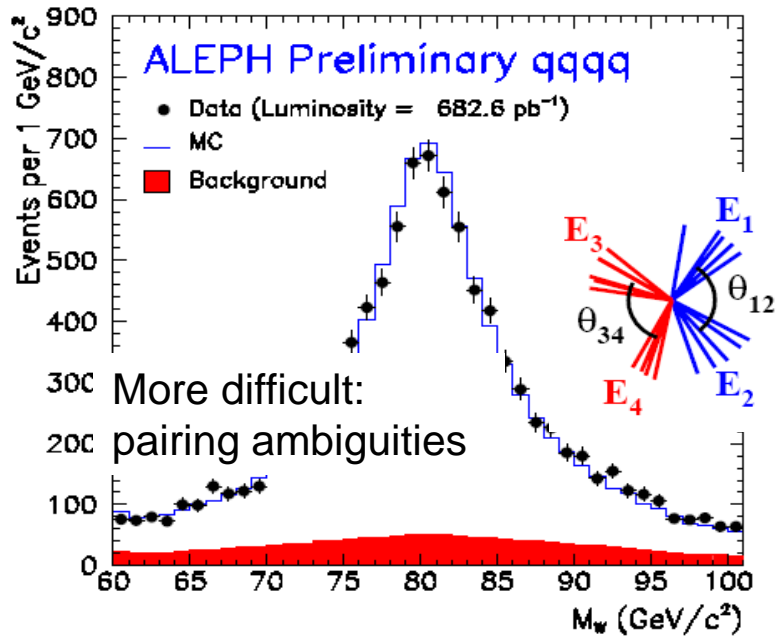
$W_1 \rightarrow l\nu$ $W_2 \rightarrow \text{JetJet}$: use JetJet invariant mass



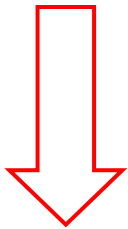
W leptonic branching fractions



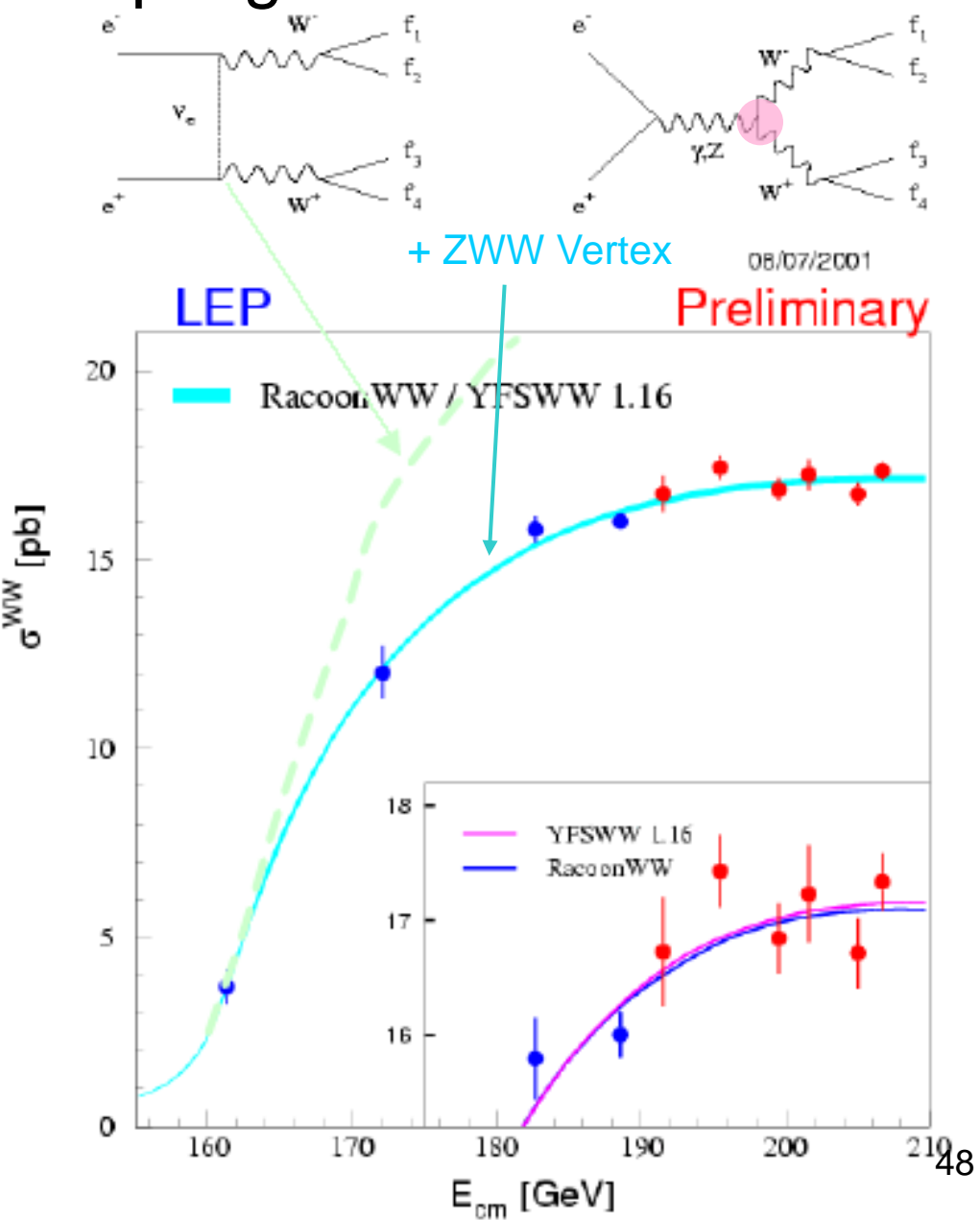
Invariant W mass reconstruction



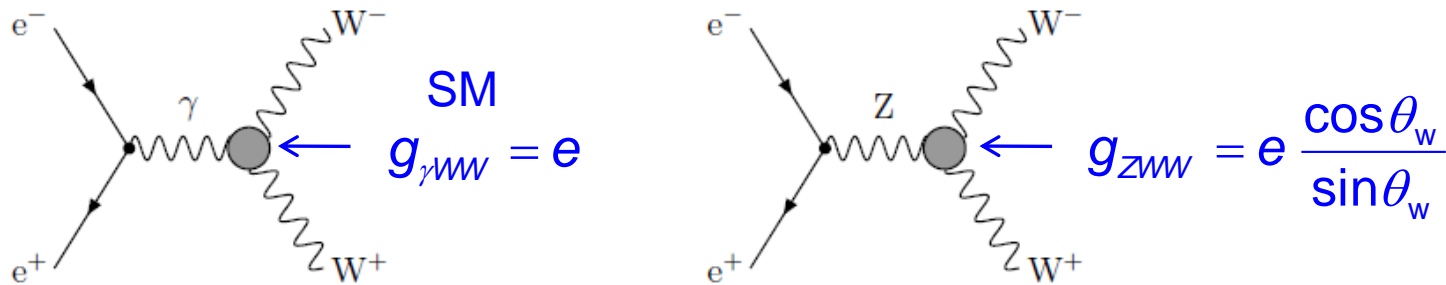
Effect of triple gauge coupling



Data confirms the existence of the γ/ZWW triple gauge boson vertex



Test of trilinear gauge boson coupling in WW production



Triple gauge coupling an important result of the non-abelian gauge structure.

Most general Lagrangian for V WW:

$$\begin{aligned}
 i\mathcal{L}_{\text{eff}}^{\text{VWW}}/g_{\text{VWW}} &= \boxed{g_1^V} V^\mu (W_{\mu\nu}^- W^{+\nu} - W_{\mu\nu}^+ W^{-\nu}) \\
 &+ \boxed{\kappa_V} W_\mu^+ W_\nu^- V^{\mu\nu} + \frac{\lambda_V}{m_W^2} V^{\mu\nu} W_\nu^{+\rho} W_{\rho\mu}^- \\
 &+ ig_5^V \varepsilon_{\mu\nu\rho\sigma} ((\partial^\rho W^{-\mu}) W^{+\nu} - W^{-\mu} (\partial^\rho W^{+\nu})) V^\sigma \\
 &+ ig_4^V W_\mu^+ W_\nu^- (\partial^\mu V^\nu + \partial^\nu V^\mu) \\
 &- \frac{\tilde{\kappa}_V}{2} W_\mu^- W_\nu^+ \varepsilon^{\mu\nu\rho\sigma} V_{\rho\sigma} - \frac{\tilde{\lambda}_V}{2m_W^2} W_{\rho\mu}^- W_\nu^{+\mu} \varepsilon^{\nu\rho\alpha\beta} V_{\alpha\beta}.
 \end{aligned}$$

$\boxed{} = 1$,
all others 0

$\Delta\kappa, \Delta g_1 \neq 0$
Deviation from SM

Interpretation for γ WW

$$\begin{aligned}
 q_W &= \pm g_V^\gamma \quad \text{charge} \\
 \mu_W &= \frac{e}{2M_W} (1 + \kappa_\gamma + \lambda_\gamma) \\
 &\quad \text{Dipol moment}
 \end{aligned}$$

W-polarization in $e^+ e^- \rightarrow W^+ W^-$

$\left. \begin{array}{l} \text{W polarization} \\ \text{Transversely: +, -} \\ \text{Longitudinally: 0} \end{array} \right\}$

TGC Parametrisation

$\Delta\lambda$	$(\lambda\lambda')$	$A_{\lambda\lambda'}^V$
1	(+, 0)	$\gamma(g_1^V + \kappa_V + \lambda_V - ig_4^V + \beta g_5^V + \frac{i}{\beta}(\tilde{\kappa}_V - \tilde{\lambda}_V))$
1	(0, -)	$\gamma(g_1^V + \kappa_V + \lambda_V + ig_4^V + \beta g_5^V - \frac{i}{\beta}(\tilde{\kappa}_V - \tilde{\lambda}_V))$
0	(+, +)	$g_1^V + 2\gamma^2\lambda_V + \frac{i}{\beta}(\tilde{\kappa}_V - \tilde{\lambda}_V)$
0	(0, 0)	$g_1^V + 2\gamma^2\kappa_V$
0	(-, -)	$g_1^V + 2\gamma^2\lambda_V - \frac{i}{\beta}(\tilde{\kappa}_V - \tilde{\lambda}_V)$
-1	(0, +)	$\gamma(g_1^V + \kappa_V + \lambda_V + ig_4^V - \beta g_5^V - \frac{i}{\beta}(\tilde{\kappa}_V - \tilde{\lambda}_V))$
-1	(-, 0)	$\gamma(g_1^V + \kappa_V + \lambda_V - ig_4^V - \beta g_5^V - \frac{i}{\beta}(\tilde{\kappa}_V - \tilde{\lambda}_V))$

Angular distribution of the corresponding helicity amplitude given by rotation matrices (d-functions): $d_{\sigma, \Delta\lambda}^{J_0}$

Electron/positron helicity: $+\sigma/2, -\sigma/2$, $J_0 = \max(|\sigma|, |\Delta\lambda|)$

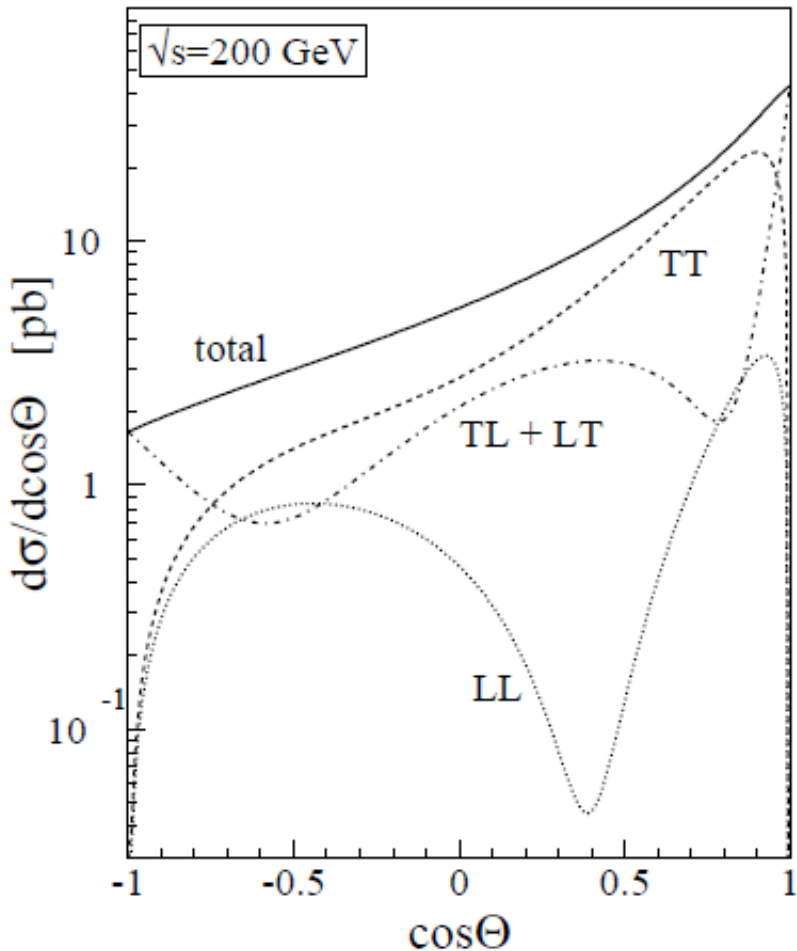


Figure 1.2: The differential cross section for the process $e^+e^- \rightarrow W^+W^-$ at 200 GeV as function of the cosine of the W^- production angle. The separate contributions from different helicity combinations of the produced W bosons are also given, with $TT= (-,+) + (+,-) + (-,-) + (+,+)$, $TL+LT= (-,0) + (+,0) + (0,-) + (0,+)$ and $LL= (0,0)$.

M.E.T. Dierckxsens, Thesis, Nijmegen, 2004

Triple Gauge couplings:

Assuming electromagnetic gauge invariance as well as C and P conservation, the number of independent TGCs reduces to five.

Common set: { g_1^Z , κ_γ , λ_Z , λ_γ }

Parameters used by the LEP experiments are: g_1^Z , κ_γ , λ_γ

With additional gauge constraints

$$\begin{aligned}\kappa_Z &= g_1^Z - (\kappa_\gamma - 1) \tan^2 \theta_W \\ \lambda_Z &= \lambda_\gamma,\end{aligned}$$

From a fit to the angular distribution of the WW:

Parameter	68% C.L.	
g_1^Z	$0.984^{+0.022}_{-0.019}$	}=1 in SM
κ_γ	$0.973^{+0.044}_{-0.045}$	
λ_γ	$-0.028^{+0.020}_{-0.021}$	

=0 in SM

Standard Model structure of VWW triple boson coupling confirmed.

4. Higher order corrections and the Higgs mass

$$\sin^2 \theta_w = 1 - \frac{M_W^2}{M_Z^2} \quad \sin \theta_w = \frac{e}{g}$$

$$\rho = \frac{m_W^2}{m_Z^2 \cos^2 \theta_w} = 1$$

$$\sin^2 \theta_W = 1 - \frac{m_W^2}{m_Z^2}$$

$$m_W^2 = \frac{\pi \alpha}{\sqrt{2} \sin^2 \theta_W G_F}$$

Lowest order
SM predictions

$\alpha(0)$

\Rightarrow

$$\bar{\rho} = 1 + \Delta\rho$$

\Rightarrow

$$\sin^2 \theta_{\text{eff}} = (1 + \Delta\kappa) \sin^2 \theta_W$$

\Rightarrow

$$m_W^2 = \frac{\pi \alpha}{\sqrt{2} \sin^2 \theta_W G_F} (1 + \Delta r)$$

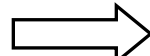
\Rightarrow

$$\alpha(m_Z^2) = \frac{\alpha(0)}{1 - \Delta\alpha}$$

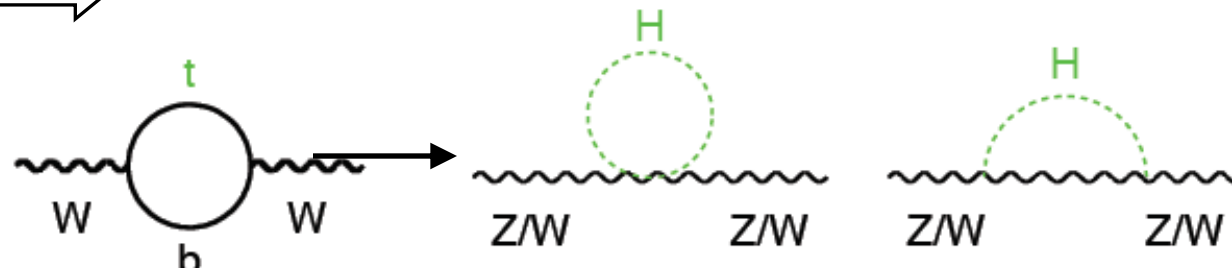
Including radiative
corrections

$$\text{with : } \Delta\alpha = \Delta\alpha_{\text{lept}} + \Delta\alpha_{\text{top}} + \Delta\alpha_{\text{had}}^{(5)}$$

$$\begin{aligned} & \sin^2 \theta_w \\ & g_A, g_V \end{aligned}$$



$$\Delta\rho, \Delta\kappa, \Delta r = f(m_t^2, \log(m_H), \dots)$$



$$\begin{aligned} & \sin^2 \theta_{\text{eff}} \\ & \bar{g}_A, \bar{g}_V \end{aligned}$$

$$\bar{g}_A = \sqrt{\bar{\rho}} T^3 \quad \bar{g}_V = \sqrt{\bar{\rho}} (T^3 - 2Q \sin^2 \theta_{\text{eff}})$$

Top mass prediction from radiative corrections

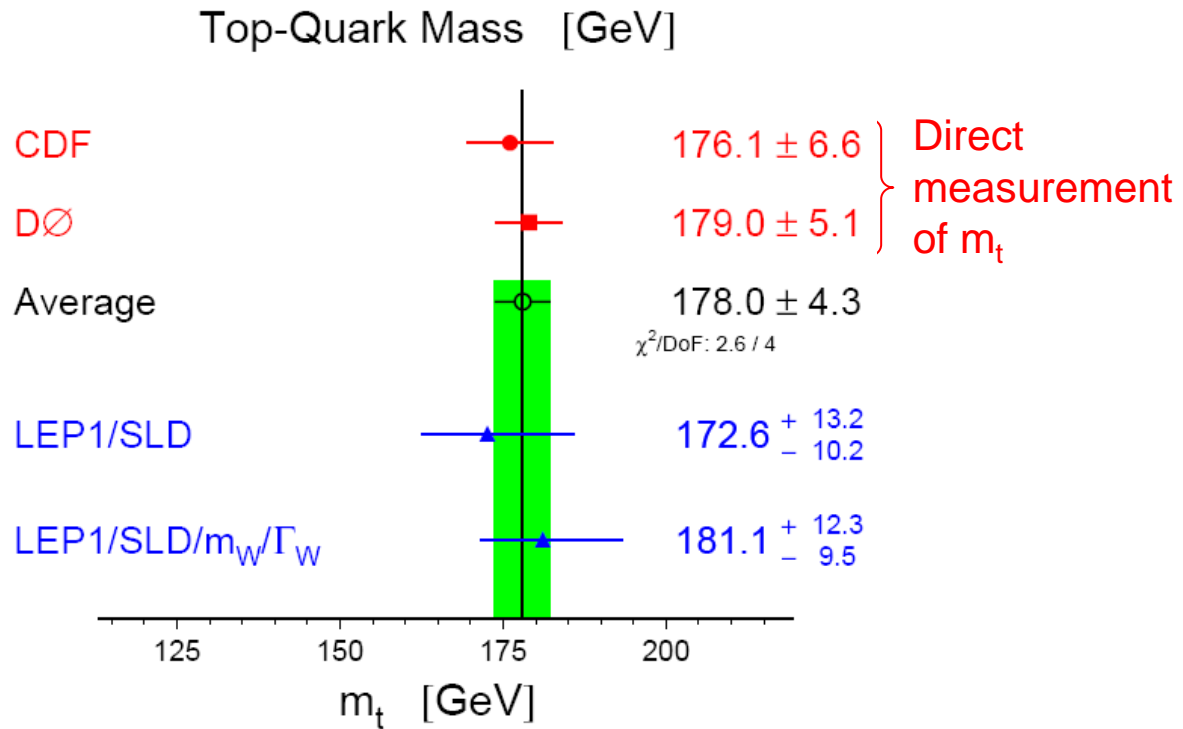
$$\text{e.g.: } \Delta r(m_t, M_H) = -\frac{3\alpha \cos^2 \theta_w}{16\pi \sin^4 \theta_w} \frac{m_t^2}{M_W^2} - \frac{11\alpha}{48\pi \sin^2 \theta_w} \ln \frac{M_H^2}{M_W^2} + \dots$$

The measurement of the radiative corrections:

$$\sin^2 \theta_{\text{eff}} \equiv \frac{1}{4} (1 - \bar{g}_V / \bar{g}_A)$$

$$\sin^2 \theta_{\text{eff}} = (1 + \Delta\kappa) \sin^2 \theta_w$$

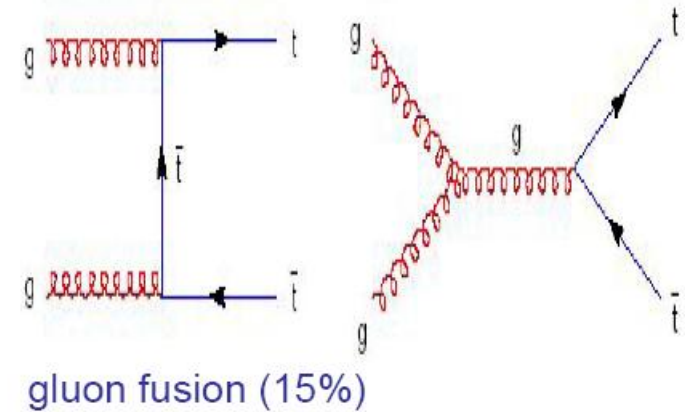
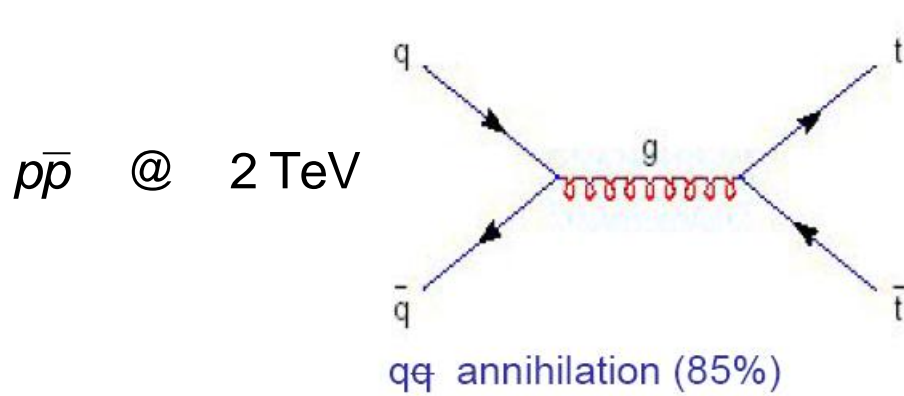
Allows the indirect determination of the unknown parameters m_t and M_H .



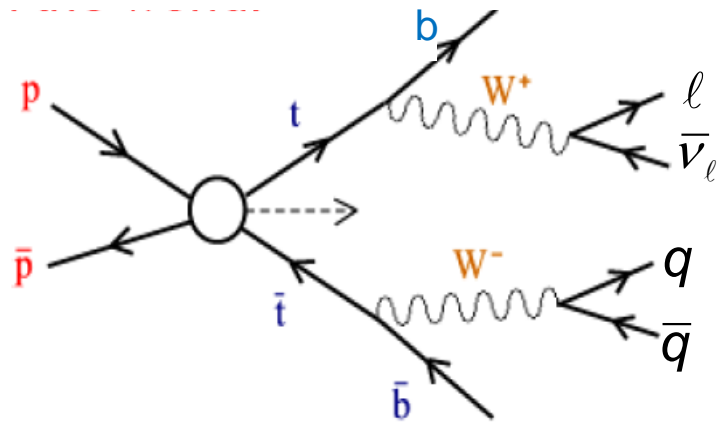
Good agreement between the indirect prediction of m_t and the value obtained in direct measurements confirm the radiative corrections of the SM

Prediction of m_t by LEP before the discovery of the top at TEVATRON.

Observation of the top quark at TEVATRON (1995)

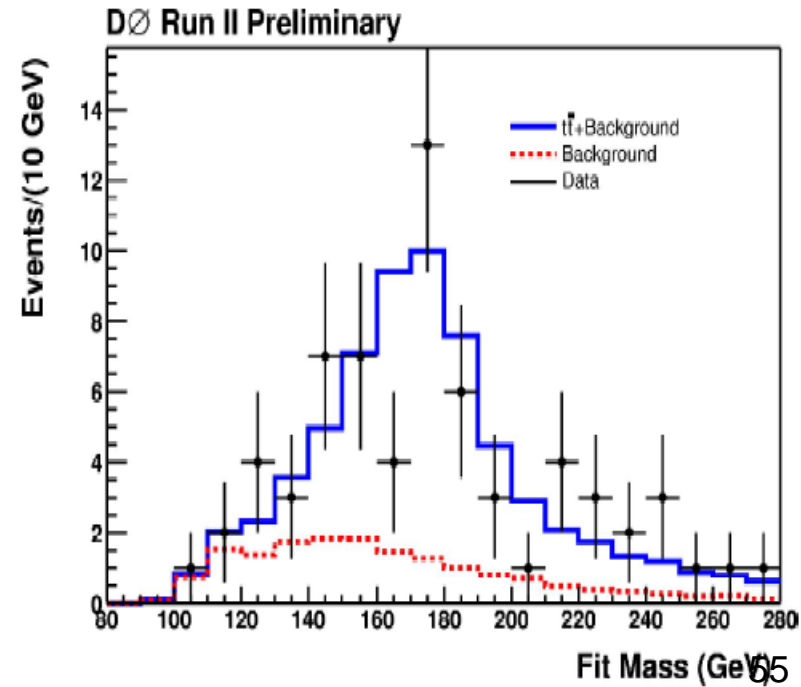


Top decay (decays before hadronization)

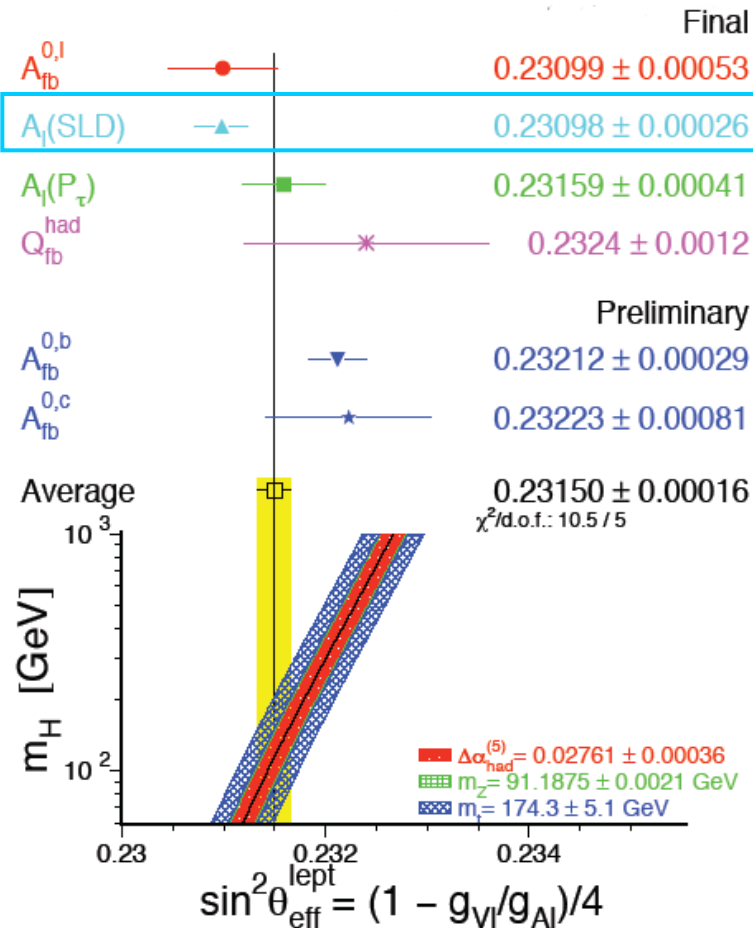


Channel used for mass reconstruction:

$$m_t = m_{inv}(b-jet, W \rightarrow jet + jet)$$



Higgs mass prediction from radiative corrections



Take the top mass from direct measurements and use the radiative corrections to determine the Higgs mass.

$$\Delta r(m_t, M_H) = -\frac{3\alpha \cos^2 \theta_w}{16\pi \sin^4 \theta_w} \frac{m_t^2}{M_W^2} - \frac{11\alpha}{48\pi \sin^2 \theta_w} \boxed{\ln \frac{M_H^2}{M_W^2}} \dots$$

Theoretical prediction of $\sin^2 \theta_{\text{eff}}$ as function of the Higgs mass.

Fits to electro-weak data:

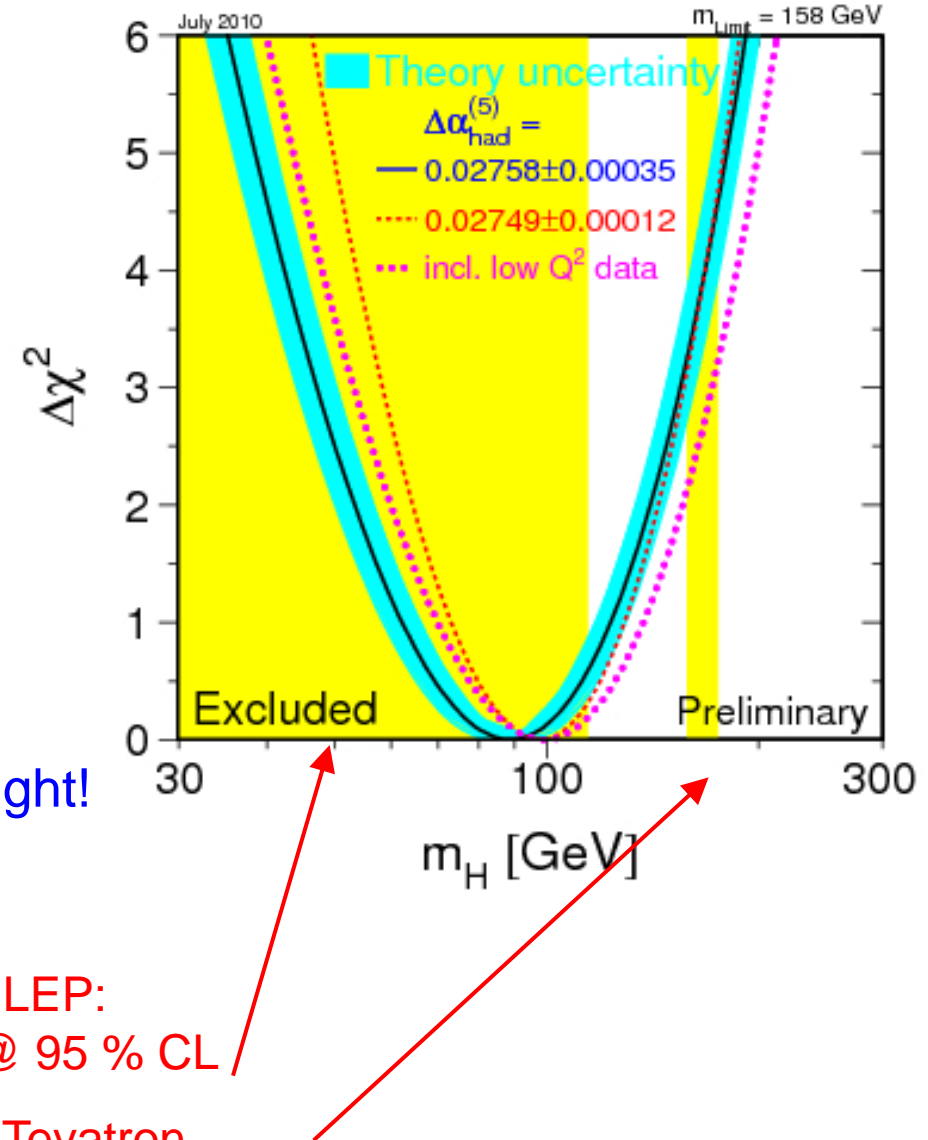
$$m_H = 89^{+35}_{-26} \text{ GeV}$$

$m_H < 158 \text{ GeV}$ (95% CL)

Assumption for fit:

- SM including Higgs
- No confirmation of Higgs mechanism

If existing, Higgs seems to be light!



- Direct searches at LEP:
 $m_H > 114.4 \text{ GeV}$ @ 95 % CL
- Direct searches at Tevatron

Unfortunately this mass region is the most difficult to explore!